The Institute of Space and Astronautical Science
Report No. 671, March 1998

The Infrared Spectra of Candidate Materials for Celestial Dust by Laboratory Measurements

By

Chiyoe KOIKE* and Hiroshi SHIBAI**

(February 5, 1998)

ABSTRACT: The optical features of various materials interesting in celestial objects were measured in wavelengths from UV to FIR region. The unpublished measured spectra of many materials were collected in this paper. These spectra are used as a clue to identify the observed spectra and study the evolution of interstellar and/or circumstellar dust.

1. INTRODUCTION

During these years, many interesting features have been observed in the spectra of various objects such as carbon-rich sources and oxygen-rich sources. In particular, crystalline silicate features have been detected in many comets (Hanner et al. 1994, and references there in) and in the circumstellar disk of β Pic (Knacke et al. 1993), since the discovery of the distinct peak at 11.25 μm in Comet/P Halley. Furthermore, recent ISO observations show that many interesting features have been detected in the dusty circumstellar disk around Oxygen rich stars (Waters et al. 1996, and references there in). These features are distinctly different from the known traditional features such as amorphous silicates, and are identified as crystal silicates such as olivine, forsterite and pyroxene.

Study of the dust existing in various sources and comparison with what we know about the interstellar and/or circumstellar dust will help to elucidate the evolution of interstellar and/or circumstellar materials.

It is evident that, in identifying these interesting features, good quantitative knowledge of optical properties of materials is required. The optical data concerning these observed spectra is still insufficient. Up to now, we measured the optical features of many materials in the wide wavelength from UV to FIR. The aim of this article is to give the measured spectra of various materials.

* Kyoto Pharmaceutical University
** Department of Physics, Nagoya University

2. EXPERIMENTAL PROCEDURE

The samples of large pieces or bulk were crushed and ground in an agate mortar, and large sized particles were removed by sedimentation. These fine particles were buried in KBr pellets or polyethylene sheets. In the mid-infrared region (2.5–25 μm), the transmissions of pellets were measured with a Shimadzu IR-27G spectrometer (2 cm^{-1} resolution at 1000 cm^{-1}) and a Fourier spectrophotometer, JASCO FT/IR-350, with 0.5 cm^{-1} resolution. In the far-infrared region (25–250 μm), the transmissions of polyethylene sheets were measured with a Fourier transform infrared spectrometer, BOMEM DA3, with 0.5 cm^{-1} resolution at Institute of Space and Astronautical Science (ISAS).

Extinction coefficients, Q_{ext}, and mass extinction coefficients, κ, are derived from the transmission T of pellets or polyethylene sheets as follows,

$$\frac{Q_{ext}}{a} = \frac{4}{3}\rho\frac{S}{M}\ln\left(\frac{1}{T}\right),$$

$$\kappa = \frac{S}{M}\ln\left(\frac{1}{T}\right),$$

where a is the particle radius of the sample, ρ is the density, S is the surface area of a KBr pellet or polyethylene sheet, and M is the mass of the sample.

Most of the present data were taken by measurements at room temperature. However, the interstellar dust and the dust in molecular clouds are in much colder temperature. So, we have made several measurements by cooling the samples; MIR spectra at 110 K and FIR spectra at 2 K. A part of these data have already been published (Koike et al. 1981a, 1982a, 1982b, 1982c). Recently, we measure the spectra of carbon and graphite samples at 4 K.

In this paper, we report the spectra of various materials interesting in celestial objects, summarizing unpublished data.

3. MEASURED SPECTRA

(1) Crystal pyroxenes and amorphous pyroxenes

The samples are listed in Table 1 and the spectra are shown in Figure 1. The peak wavelengths are listed in Tables 2 and 3.

(2) Olivine and pyroxene

Olivine and pyroxenes were collected from Ichinome-gata, Akita. Far-infrared spectra were measured at room temperature (Koike et al. 1993), mid-infrared spectra at 110 K (Koike et al. 1981a), and far-infrared spectra at 2 K (Koike et al. 1982a,b). The results are shown in Figures 2, 3, and 4.

(3) Hydrous silicates

For the typical hydrous silicates, serpentine, chlorite, and montmorillonite were selected. The far-infrared spectra at 2 K (Koike et al. 1982c) and at room temperature (Koike et al. 1990) are shown in Figure 5.

(4) Silicon carbide

The measured spectra of various types of silicon carbide are shown in Figure 6 (Koike 1987). α-SiC samples are commercially available and β-SiC samples were made up in the laboratory. The

results of the measurements are listed in Table 4.

(5) Carbon and graphite

The measured samples are listed in Table 5. The samples are measured in a wide wavelength range (UV to FIR) at room temperature. The spectra are shown in Figure 7 (Koike et al. 1996). The correlation between the optical properties and the degree of crystalization is shown in Table 6. Koike et al. (1996) reported, in the far-infrared region, the spectral index increases as the degree of crystalization which was directly observed with a transmission electron microscope (TEM). These samples are also measured at 4 K in the far-infrared region, and the results are shown in Figure 8.

(6) Oxidized metals

The oxidized iron samples, magnetite (Fe_3O_4) and hematite (Fe_2O_3), were measured in the far-infrared region as shown in Figure 9. The recent results are indicated by lines and those of the previous measurement (Koike et al. 1981b) by filled circles ("old fir") in Fig. 9. The spectra cooled down at 2 K are previous data (Koike et al, 1982a,b). A remarkable variation of the magnetite spectra in the far-infrared region can be seen, probably due to variation of aggregation degree in individual sheets. On the other hands, we cannot see any remarkable variation of the hematite spectra.

The spectra of calcite ($CaCO_3$) samples are shown in Figure 10, compared with those of the bulk sample (Hellwege et al. 1970). The bulk spectra are derived by three methods; (a) the average of Q_{ext} of each optical axis, (b) the Q_{ext} from the average of n, k, and (c) the Q_{ext} from the average of ε_1, ε_2 (Suto et al. 1992), where $\varepsilon_1=n^2-k^2$, and $\varepsilon_2=2nk$.

The spectra of titan (TiO_2) -A and -B, are shown in Figure 11. The samples are commercially available and these average diameters are 40–50 nm. The sample A is Rutil and sample B is Anatase. The measured spectra from UV to NIR probably have large errors.

(7) Meteorites (Murchison and Allende meteorites)

The spectra of Murchison from which the white inclusion had been removed were measured after annealing at 200–1400°C. The results are shown in Figure 12 (a) (b) (Koike et al. 1983). The spectrum gradually changes as the annealing temperature, and becomes similar to that of Allende shown in Figures 12(c) and (d). The spectrum of Allende was not so much changed as the spectrum of Murchison by annealing even at high temperatures. Figure 12(c) shows the spectrum of original fine grains of Allende (density < 3.86 g/cm^3) by the solid line with that of Murchison (not annealed) by the dotted line. Figure 12(d) shows the spectra of Allende 2–4. They are the samples selected with an isodynamic separator; the density was determined to be 3.75 g/cm^3 by the heavy liquid sedimentation method (Koike et al. 1993).

4. ACKNOWLEDGEMENTS

We thank Professor Haruyuki Okuda at ISAS for his continuous encouraging to us in all of this work, and thank Professor Akira Fujiwara for his careful reading of this paper. We thank all members of the infrared group at ISAS for helping us with the far-infrared extinction measurements.

REFERENCES

M. S. Hanner, D. K. Lynch, and R. W. Russell, 1994, "The 8–13 Micron Spectra of Comets and the Composition of Silicate Grains", Astrophys. J., 425, 274–285.

K. H. Hellwege, W. Lesch, M. Plihal, and G. Schaack, 1970, "Zwei-Phononen-Absorptionsspektren und Dispersion der Schwingungszweige in Kristallen der Kalkspatsruktur", Z. Physik, 232, 61–86.
R. F. Knacke, S. B. Fajardo-Acoster, C. M. Telesco, J. A. Hackwell, D. K. Lynch, and R. W. Russell, 1993, "The Silicates in the Disk of β Pictoris", Astrophys. J., 418, 440–450.
C. Koike, T. Maihara, and H. Hasegawa, 1981a, "The Mid-Infrared Spectrum of High Temperature Silicate Minerals Cooling on Low Temperature", in Proc. 14th ISAS Lunar & Planet. Sympo., 14, 149–155.
C. Koike, H. Hasegawa, N. Asada, and T. Hattori, 1981b, "The extinction Coefficients in Mid- and Far-infrared of Silicates and Iron-oxide Minerals of Interest for Astronomical Observation", Astrophys. Sp. Sci., 79, 77–85.
C. Koike, 1982a, "The Measurements of Absorption Coefficients of Astronomical Dust at Low Temperature" (Japanese), in Proc. "Evolution of Solar System and Planetary Environments", 122–126.
C. Koike, H. Hasegawa, and T. Hattori, 1982b, "The Far-Infrared Extinction Coefficients of Minerals at Low Temperature", in Proc. 15th ISAS Lunar & Planet. Sympo., 15, 114–119.
C. Koike, H. Hasegawa, and T. Hattori, 1982c, "Mid- and Far-Infrared Extinction Coefficients of Hydrous Silicate Minerals", Astrophys. Sp. Sci., 88, 89–98.
C. Koike and Y. Tazawa, 1983, "Thermo-Metamorphyism of the Murchison and Allende Meteorite", in Proc. 16th ISAS Lunar & Planet. Sympo., 16, 89–92.
C. Koike, 1987, "The Infrared Absorption of SiC" (Japanese), in Grain Formation Work Shop, VIII, 48–52.
C. Koike and H. Shibai, 1990, "Optical Constants of Hydrous Silicates from 7 to 400 μm", Mon. Not. R. astr. Soc. 246, 332–336.
C. Koike, H. Shibai, and A. Tuchiyama, 1993, "Extinction of Olivine and Pyroxene in the Mid and Far Infrared", Mon. Not. R. astr. Soc., 264, 654–658.
C. Koike, H. Suto, H. Sogawa, H. Shibai, C. Kaito, D. Ban, T. Tanabe, and Y. Ando, 1996, "The Absorption of Carbon and Graphite Particles in the Wavelengths from UV to Far Infrared", in Proc. 29th ISAS Lunar & Planet. Sympo., 29, 56–59.
T. Mukai, 1990, "Cometary Dust and Interplanetary Particles", in Evolution of Interstellar Dust and Related Topics, 397–445.
H. Suto, C. Koike, and H. Shibai, 1992, "Comparison of Approximation Methods with the Measurements of Extinction of Fine Particles in the Infrared Region", in Proc. 25th ISAS Lunar & Planet. Sympo., 25, 255–261.
T. Tanabe, Y. Nakada, F. Kamijo, and A. Sakata, 1983, Publ. Astron. Soc. Japan, 35, 397.
L. B. F. M. Waters et al., 1996, "Mineralogy of Oxygen-Rich Dust Shells", Astron. Astrophys., 315, L361–L364.

Table 1. Crystalline and amorphous pyroxene samples used in the present study.

Sample	Chemical composition	Crystal system	Natural/Synthetic
Clinoenstatite	$MgSiO_3$	monoclinic	Flux-grown/reheated
Orthoenstatite	$MgSiO_3$	orthorhombic	Flux-grown
Orthopyroxene	$En_{89.9}Fs_{8.9}Wo_{1.2}$	orthorhombic	Bambel, Norway
Diopside	$Wo_{46}En_{64}$	monoclinic	CZ-grown
Enstatite glass	$MgSiO_3$	amorphous	Quenched melt
Enstatite gel	$MgSiO_3$	amorphous	Sol-gel method
Diopside glass	$CaMgSi_2O_6$	amorphous	Quenched melt

Table 2. The peak wavelengths of present crystalline samples in medium (μm).

Synthetic enstatite		Orthopyroxene		Diopside	Augite
Clino-enstatite†	Ortho-enstatite	Natural Norway	Natural Ichinome	synthetic†	Natural Ichinome
		7		7.14	
			9.30	**9.39**	**9.30**
9.46	**9.48**				
		9.62			
10.0	9.97	**9.95**			
			9.9*		
10.5*	10.5*		**10.58**	**10.42**	**10.26**
10.83	**10.87**	**10.87**			
			11.17	11.0*	
11.29*	11.24*	11.3*			**11.36**
			11.63	**11.56**	
11.83	**11.83**	**11.74**			
		12.7*			
			13.89		
14.03	13.99	13.95			
	14.64		14.54		
		14.71			
14.93					14.93
		15.15		15.04	
15.67	15.65	15.67	15.63	15.95	15.75
18.2*	18.2*	18.2*			
18.9*		18.9*	18.7		**19.23**
	19.69	**19.61**	**19.61**		
20.0				**20.0**	
21.05				**20.9**	**20.62**
	21.74	**21.37**	21.74		
22.22					
23.23					
	24.69	25.1		**25**	25
26.5					
28.1	26.6				
	28.6	**28.4**	**28.5**		
	29.3			**29.4**	**29.5**
					32.3
33.1	**33.0**	33.7		**33.3**	33.7
35.5					
	36.0	**36.5**	**36.2**		
	40.8				**39.9**
	43.2	**43.9**	**44**		
	49.0	50*			
	51.6				
	68.6	**72.0**			**66.2**
	72.8	**74.6**			

Bold number: strong peak wavelength
*: very weak peak
†: spectra longer than 40 μm are not measured.

Table 3. The peak positions of amorphous pyroxenes in medium (μm).

Diopside-glass		Enstatite-glass		Enstatite-gel	
starting†	hydration†	starting	hydration†	Starting	hydration†
7.04	6.80			7.02	6.94
10.21	9.90	10.42	10.21	10.05	10.0
	11.8*				
	12.2*				
14.29	14.20*				
	15.27*		16.0*	15.63*	15.39
20		19.23			
	21.74		21.74	21.41	21.74
30.86	31.25				32*
				45*	

*: weak peak
†: spectra longer than 40 μm are not measured.

Table 4. The results of SiC samples.

	d (diameter)	λp(μm) (peak wavelength)	κ (cm^2/g)	crystal type (by x-ray and electron diffraction)
α-SiC				
Toshiba SiC A-1	0.38 μm	11.76	1.879(4)	α(6H)
Ibiden SiC-B	0.27 μm	11.76	1.507(4)	α(6H), Si
β-SiC				
AO-8	8 nm	12.20	1.163(4)	β
AO-15	15 nm	12.15	9.553(3)	β
AO-30	30 nm	12.15	1.125(4)	β
AO-35	35 nm	11.36	9.988(3)	21R
AO-45	45 nm	11.36	1.394(4)	21R

Table 5. The samples of carbon and graphite.

Amorphous Carbon		
Commercial		
Phil black E (P.B.E.)	297±92 Å (150–650 Å)	
Seast F	694±328 Å (100–1400 Å)	
Miike #20	1860±550 Å (1000–4000 Å)	
Laboratory		
A-A	direct heating of carbon rod in CH_4-gas (200 Torr)	
A-B	arc striking between carbon rods in CH_4-gas (300 Torr)	
A-C	direct heating of carbon rod in C_6H_6-gas (40 Torr)	
A-D	arc striking between carbon rods in C_6H_6-gas (80 Torr)	
BE	lamp-black from benzene in air	
XY	lamp-black from xylene in air	
TU	made by an arc in Ar-gas	
Graphite Commercial		
Nihon Kokuen	T-1 (Dojou)	1.1 μm
	USSP (0.5 μ)	0.5 μm
	CSSP (1.0 μ)	1.0 μm
	J-ACP (Rinjou)	3.2 μm
Ultra Carbon	UCP-1-M	< 1 μm
	1-M-USP	< 1 μm
Lonza	KS2.5	2–3 μm
	T10	~10 μm

Table 6. The correlation between the spectral index (mid infrared, far infrared) and the degree of crystallization of various carbon and graphite samples.

	d	β (mir)	β (at λ ~100 μ)	size of microcrystallites	**Crystallizations**
					wrong ↑
Carbon					
A-C	~250 Å	0.73	0.62 (0.55–0.62)	15 Å (10–25 Å)	
XY	100–300 Å	0.8	0.70	10–16 Å	
BE	300–700 Å	0.94	0.80	15–30 Å	
A-D	~450 Å	0.70	0.78 (0.67–0.78)	30 Å	
P.B.E.	297 Å	0.70	0.83 (0.75–0.87)	30 Å	
A-A	200–300 Å	0.68	0.75 (0.75–0.89)	50–60 Å, rods, needle, plate	
A-B	~750 Å	0.72	0.89 (0.65–0.89)	80–200 Å, nano tube	
Seast F	694 Å	0.88–0.72	0.93 (0.84–0.93)	40 Å, onion-like	
Miike	1860 Å	1.1 (1.1–0.97)	1.28 (1.0–1.4)	onion-like	
Graphite					
Dojou	1.10 μ		1.8 (1.8–1.9)	plate, AC (Amorphous Carbon)	
0.5 μ	0.5 μ		1.9 (1.8–1.9)	plate, AC, tube, curled whisker	
1.0 μ	1.0 μ		1.9 (1.9–2.0)	plate, AC, tube	
KS 2.5	2–3 μ		2.2 (2.2–2.4)	plate	
UCP-1-M	<1 μ		2.3 (2.2–2.4)	plate	
1-M-USP	<1 μ		2.6 (2.4–2.8)	plate	
Rinjou	3.2 μ		2.75 (2.5–2.9)	plate	
T10	~10 μ		2.9 (2.7–3.4)	plate	**good** ↓

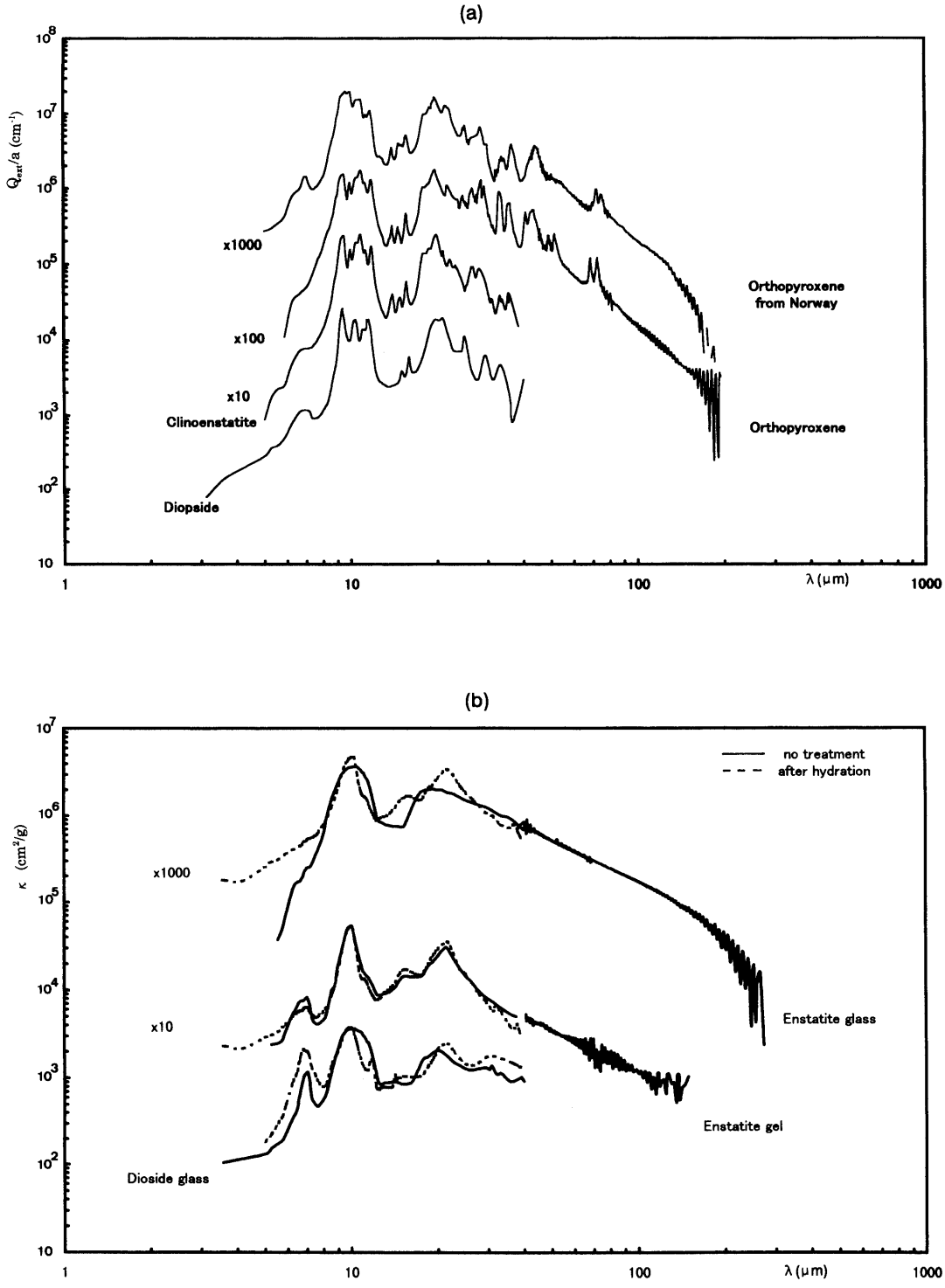

Fig. 1: (a) The extinction coefficient spectra of pyroxenes divided by the particle radius, a. (b) The mass extinction cross-section of amorphous pyroxenes. Dashed lines indicate those after hydration.

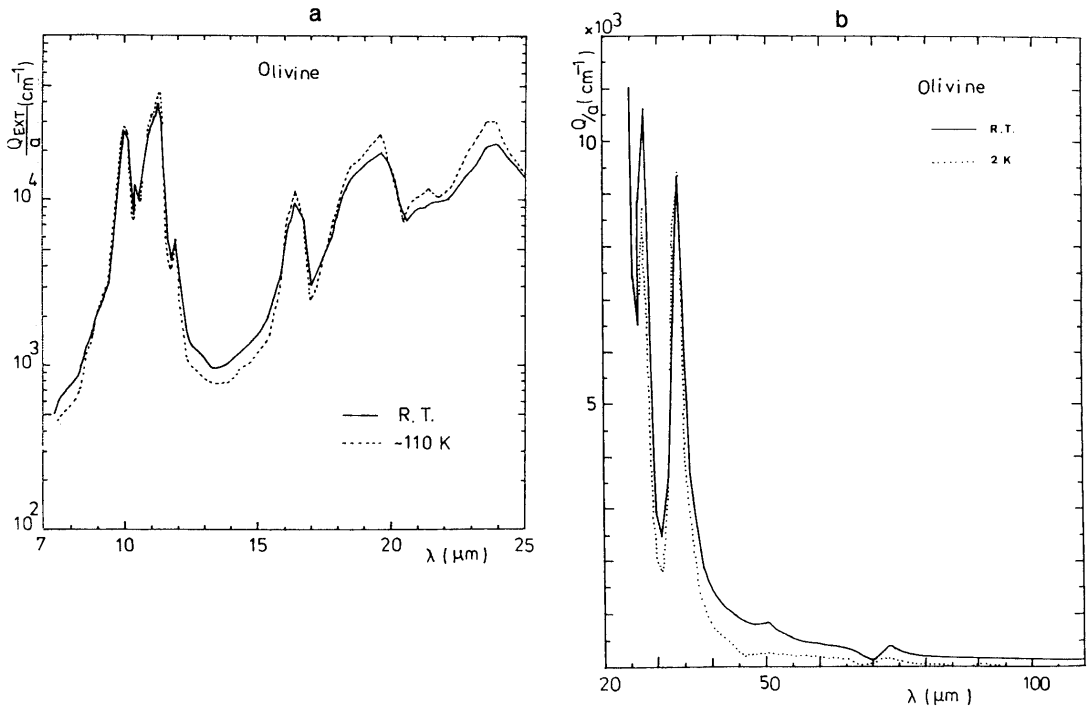

Fig. 2: The extinction coefficient spectra of olivine. (a) at room temperature compared with those cooled down to 110 K in the mid-infrared region, and (b) at 2 K in the far-infrared region.

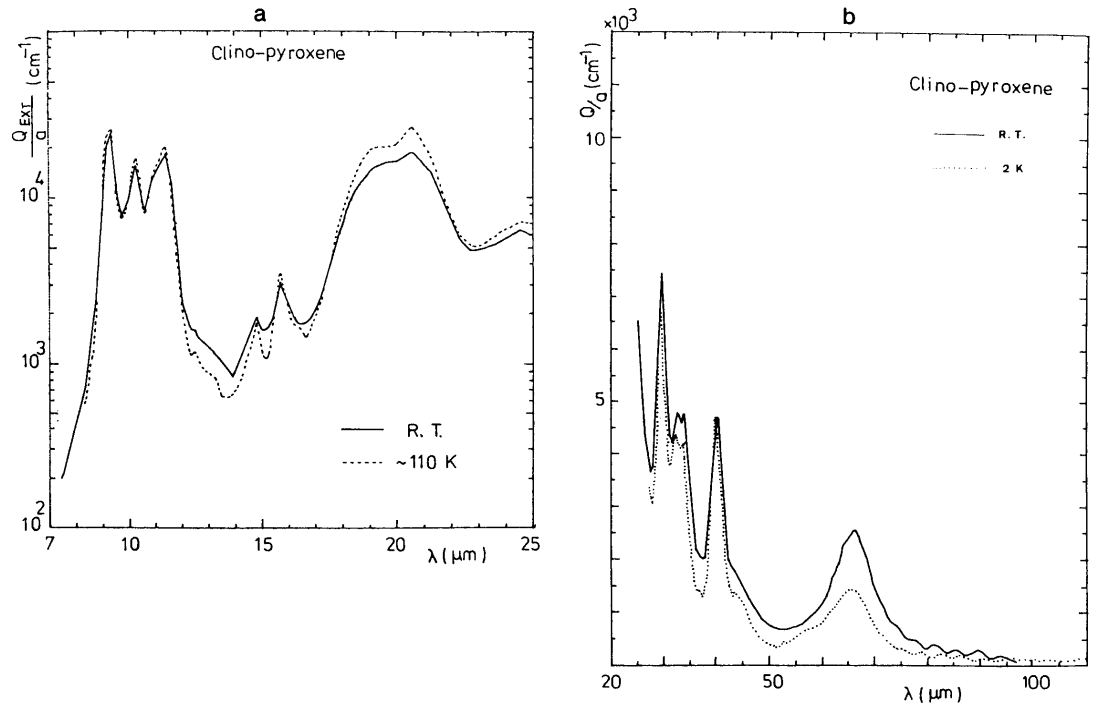

Fig. 3: The same as Figure 2 for clino-pyroxene.

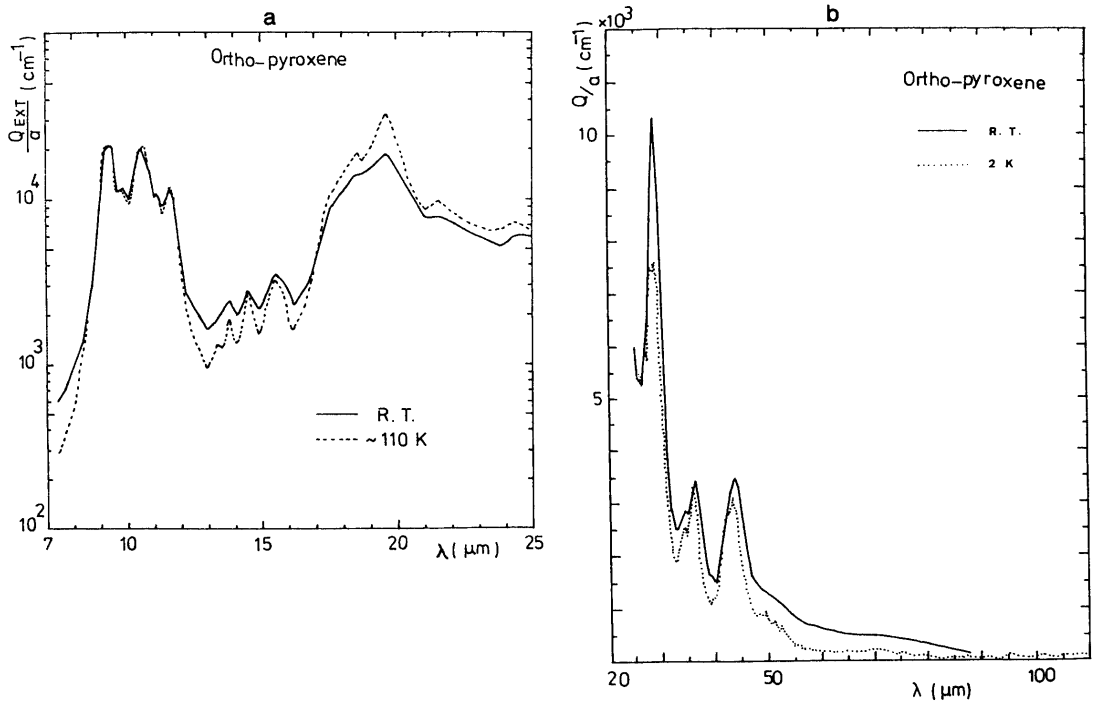

Fig. 4: The same as Figure 2 for ortho-pyroxene.

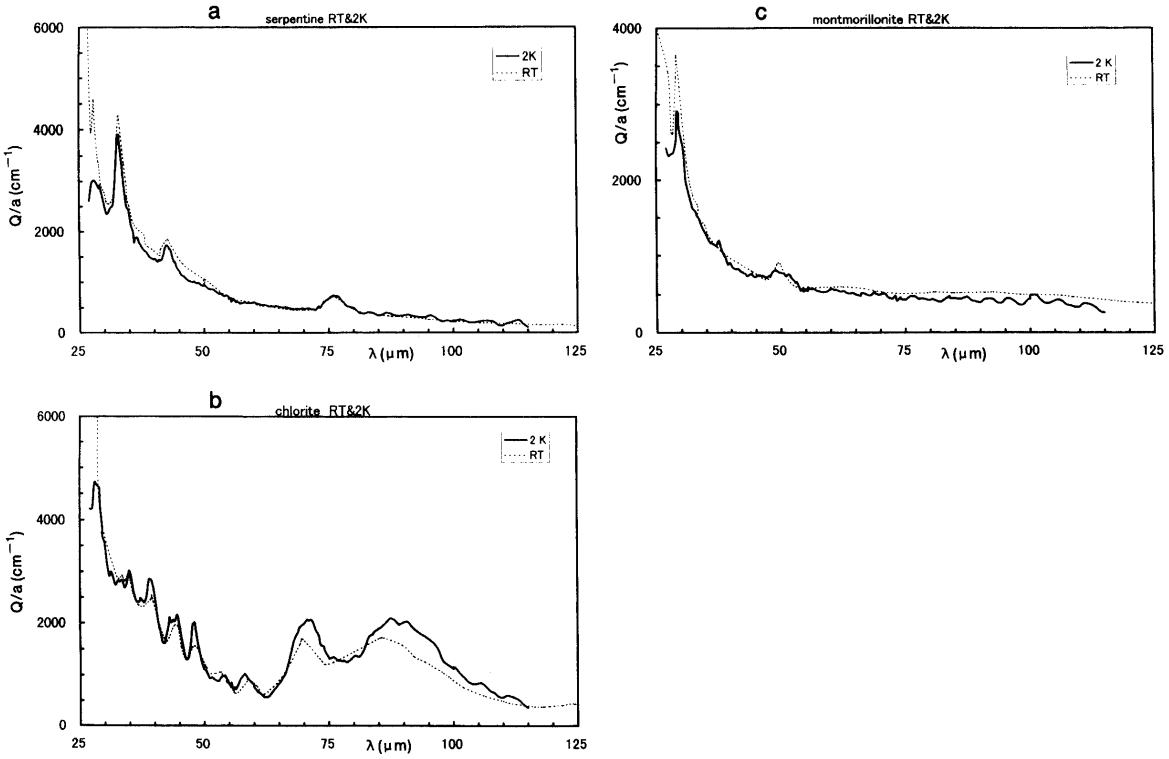

Fig. 5: The extinction coefficient spectra of (a) serpentine, (b) chlorite, and (c) montmorillonite at room temperature and at 2 K in the far-infrared region.

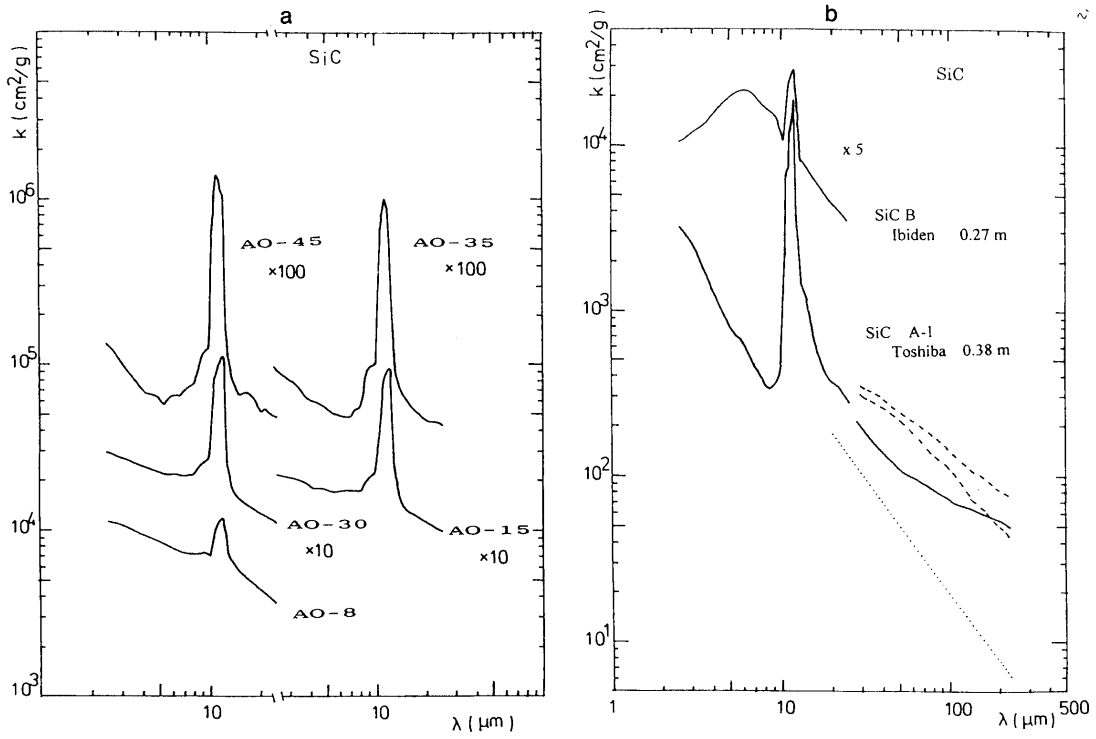

Fig. 6: The mass extinction cross-section spectra of (a) β-SiC in the mid-infrared region, and (b) α-SiC in the mid- and far-infrared region. See Table 4 for sample identifications. The dashed lines in (b) indicate the extinction cross-section spectra of SiC A-1 by old and unsettled measurements, and the dotted line in (b) is the extinction cross-section spectrum of β-SiC measured by Tanabe et al. (1983).

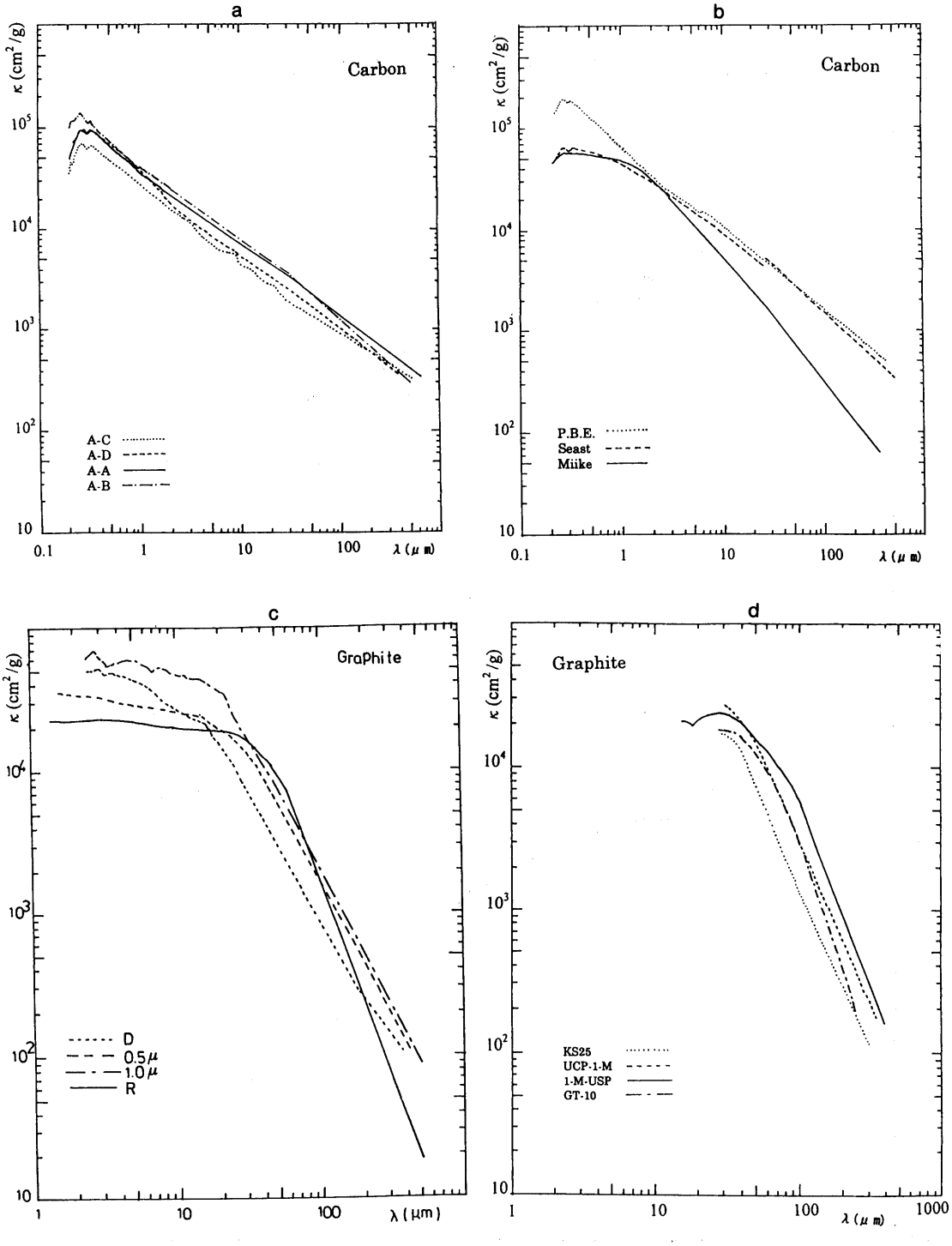

Fig. 7: The mass extinction cross-section spectra at room temperature of (a) amorphous carbon samples produced in the laboratory, (b) commercially available amorphous carbon samples, (c) commercially available graphite samples in Japan and (d) imported samples. See Table 5 for sample identification.

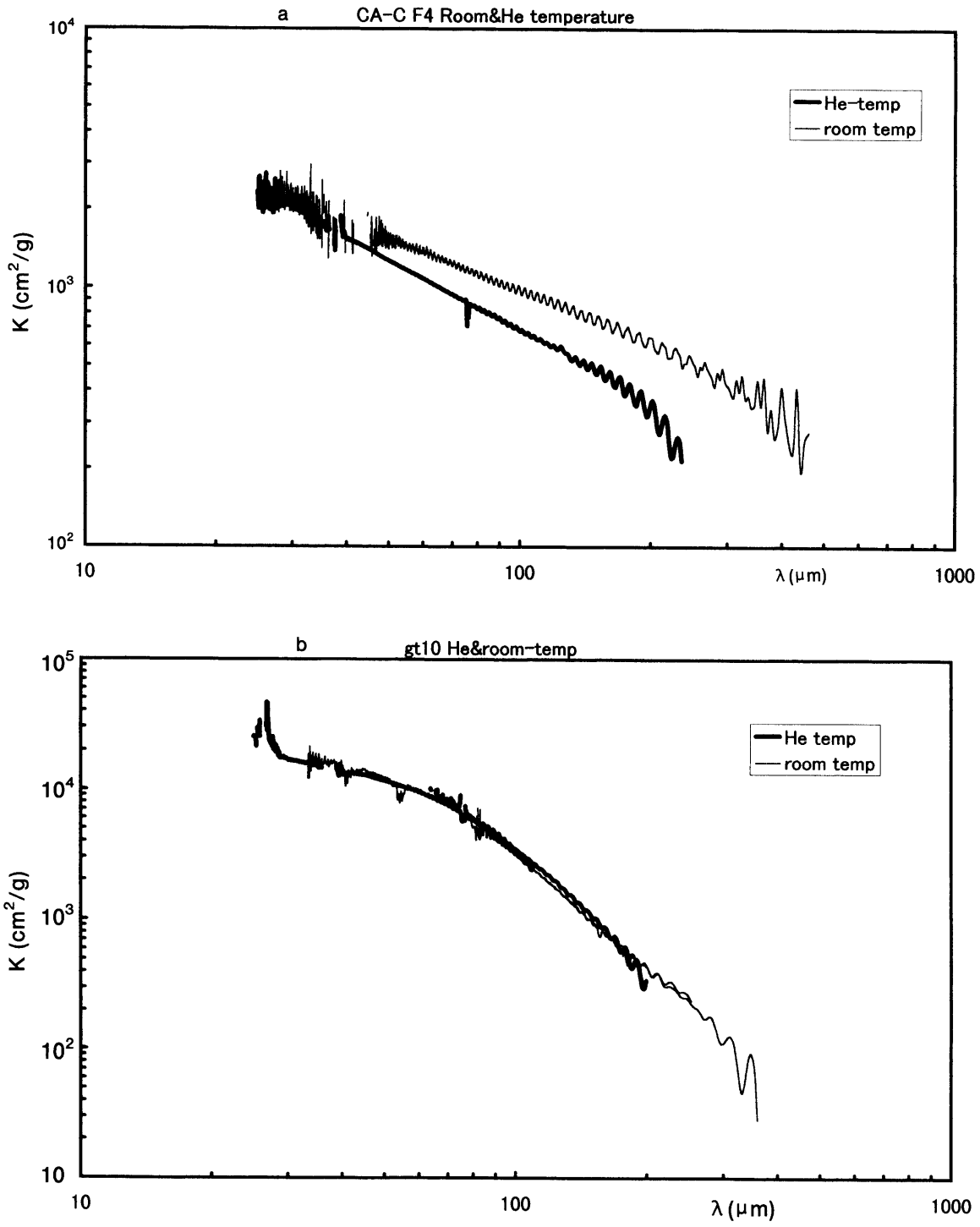

Fig. 8: The mass extinction cross-section spectra of (a) amorphous carbon (CA-C) and (b) graphite (gt10) at 4 K (thick lines) and at room temperature (thin lines).

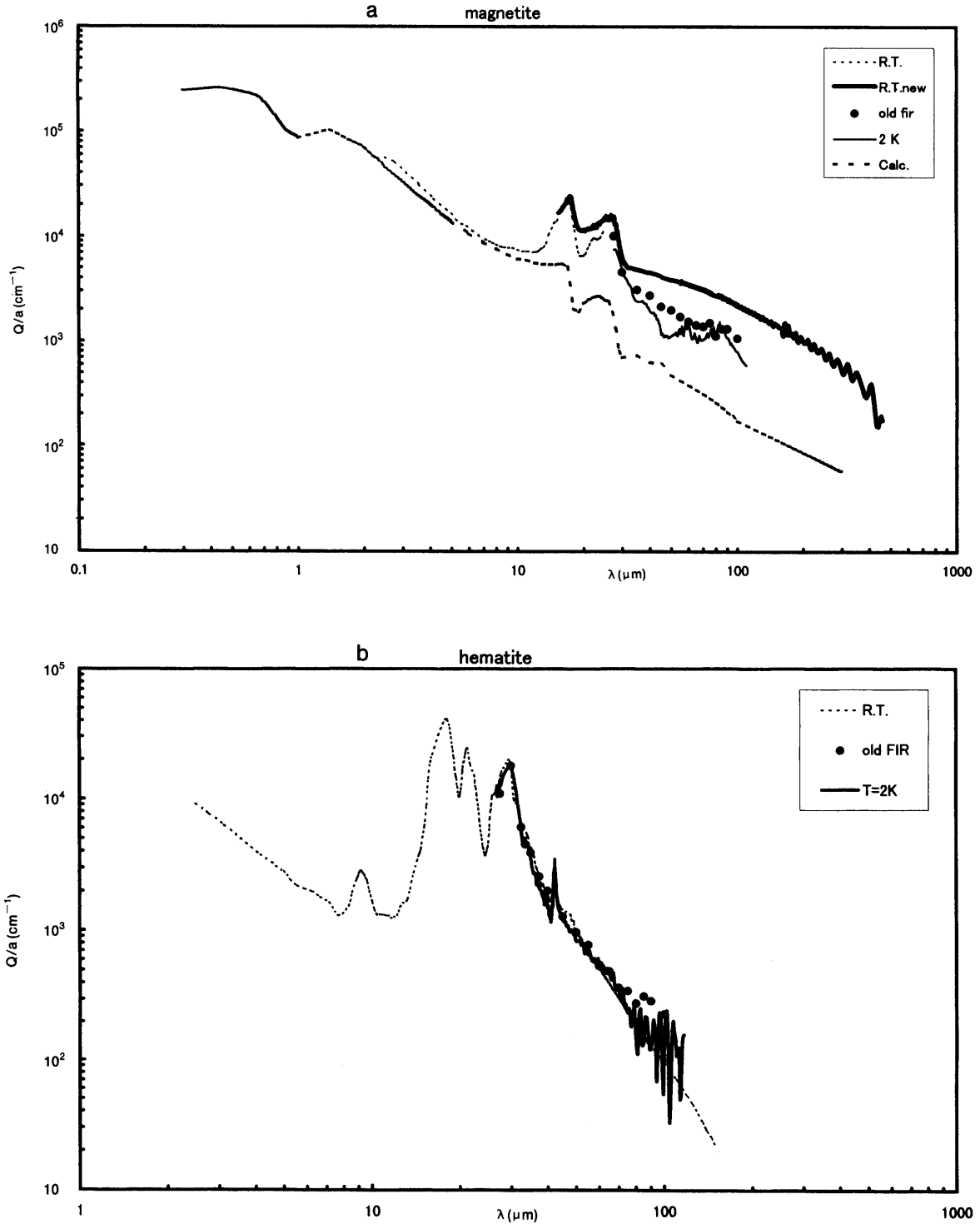

Fig. 9: The extinction coefficient spectra of (a) magnetite and (b) hematite at room temperature and at 2 K. In the panel (a), the theoretical spectra (Mukai 1990) is also shown.

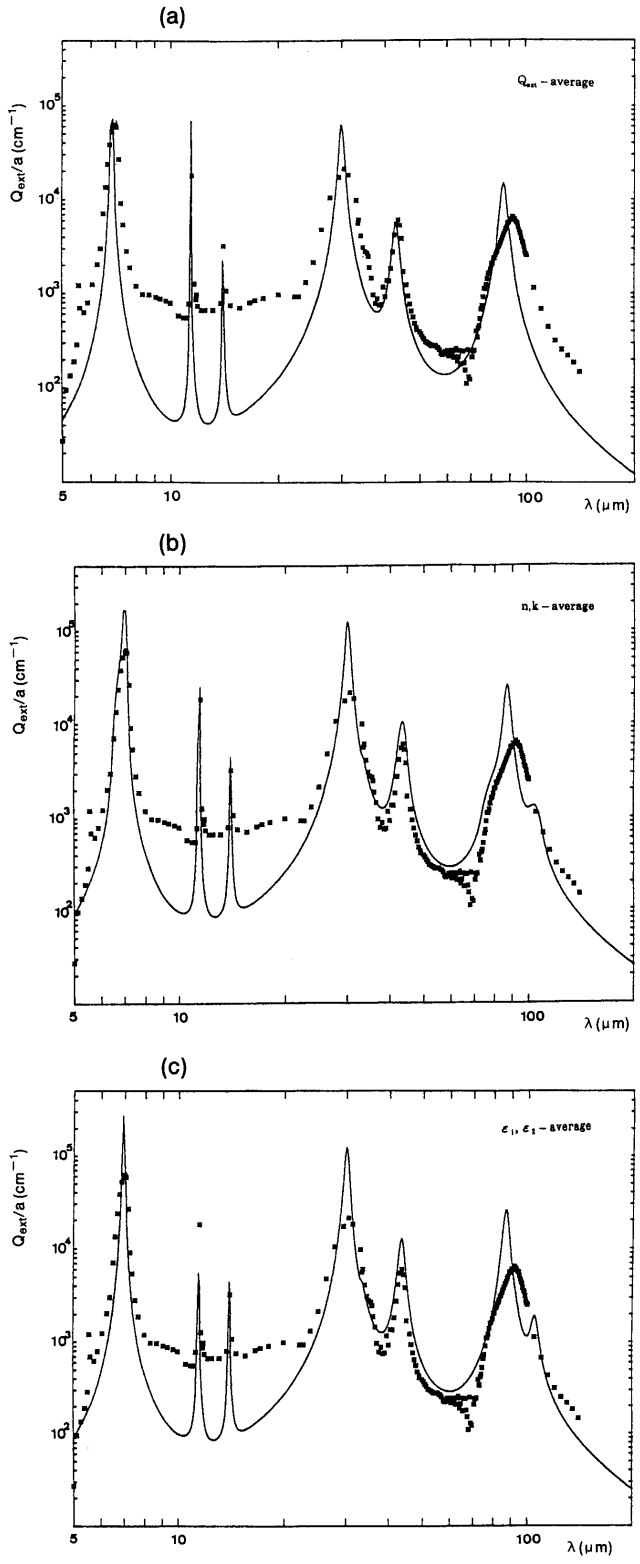

Fig. 10: The extinction coefficient spectra of Calcite compared with (a) theoretical spectra of average Q_{ext}, (b) those from average n and k, and (c) those from average ε_1, ε_2.

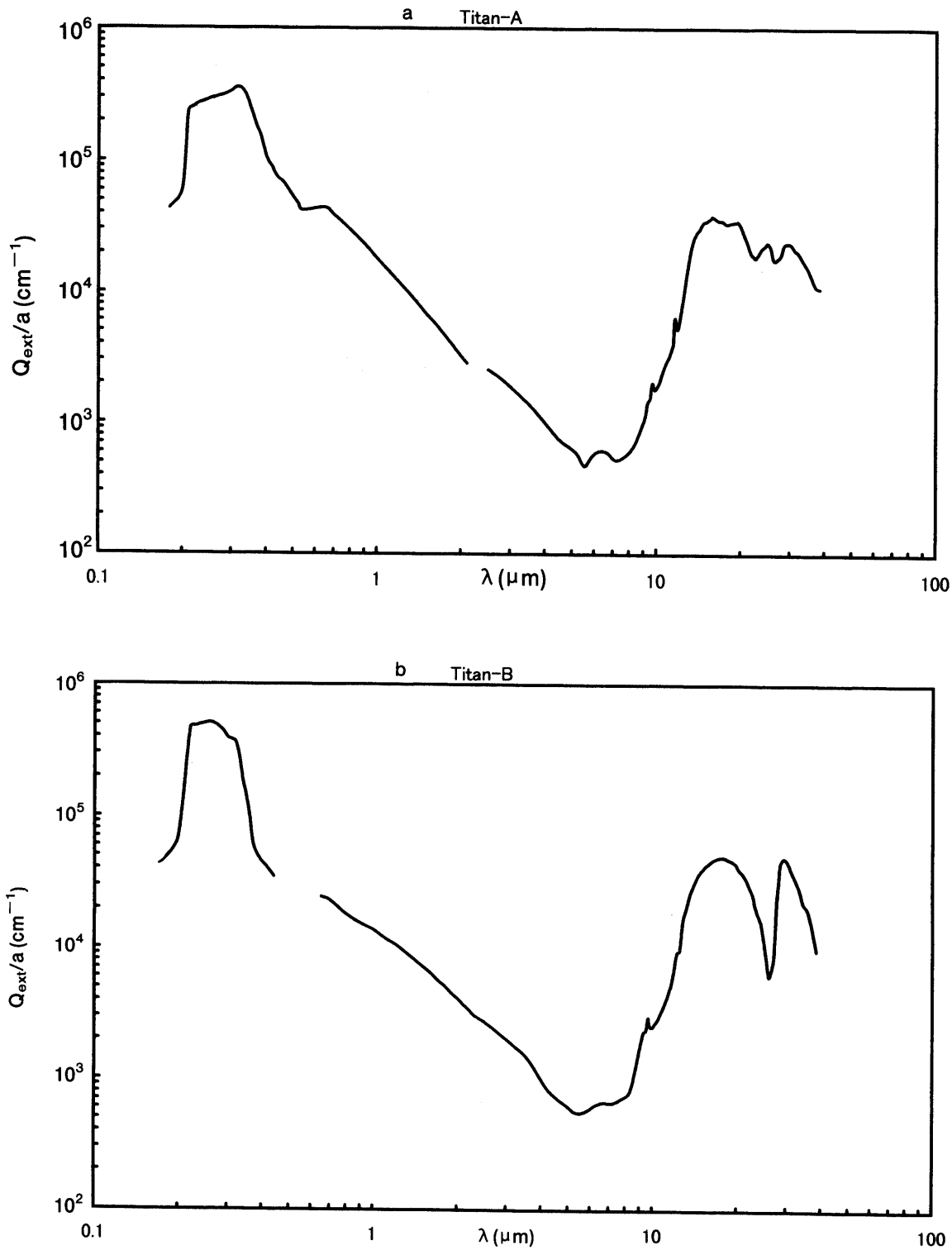

Fig. 11: The extinction coefficient spectra of (a) Titan - A (Rutil) and (b) Titan - B.

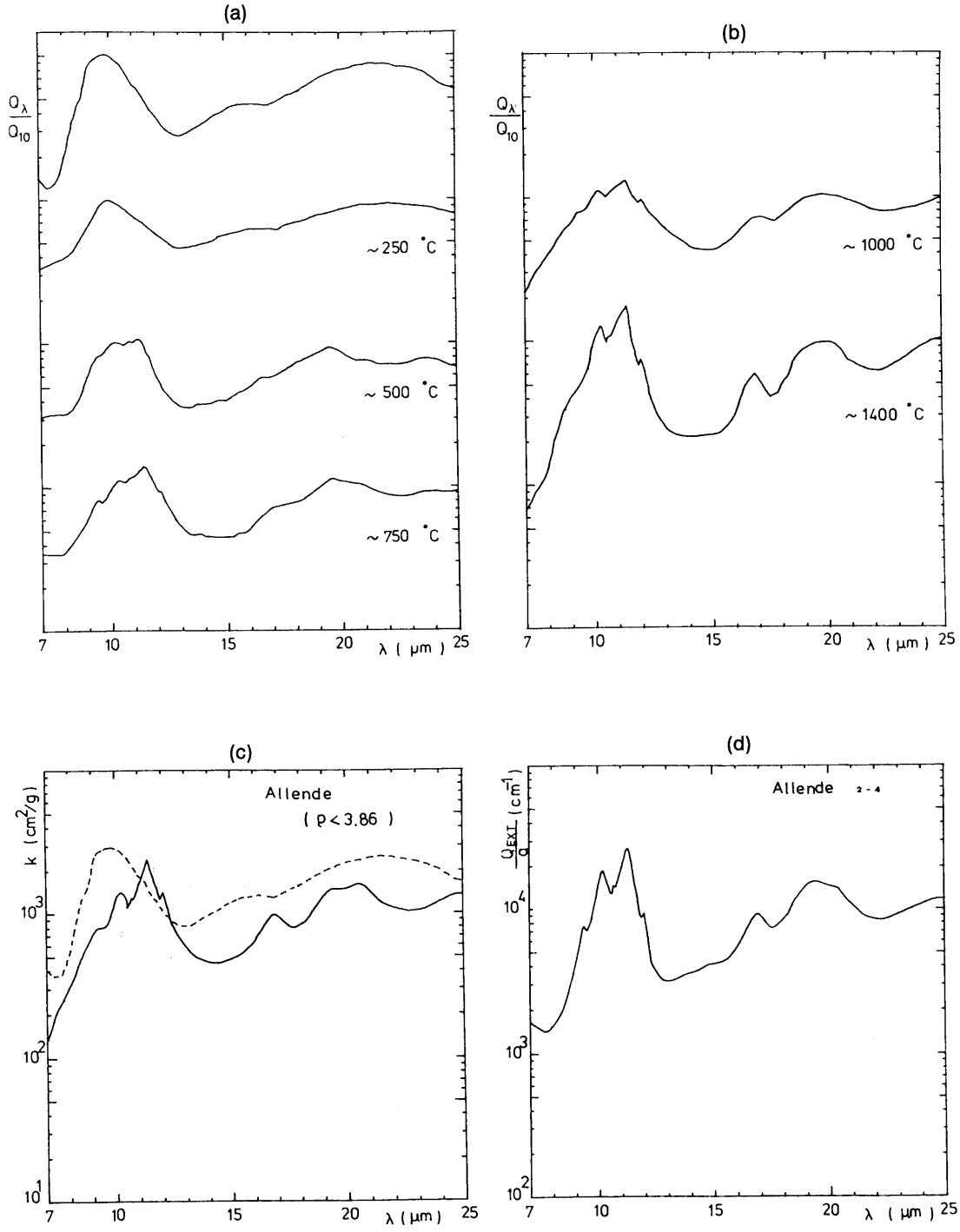

Fig. 12: The extinction coefficient spectra of (a) (b) Murchison annealed at 250–1400°C in an arbitary scale, (c) unannealed Allende (density < 3.86 g/cm^3) in a solid line and unannealed Murchison in dashed line, and (d) Allende collected with an isodynamic separator (Koike et al. 1993).